# Advances in diamond generating for 8.4 meter telescope mirrors

Johnathan M. Davis, Hubert M. Martin, Dae Wook Kim, Adrian R. Loeff, Kurtis L. Kenagy,
Raymond W. Sisk, Jeffrey R. Hagen
Steward Observatory, University of Arizona

## ABSTRACT

The Richard F. Caris Mirror Lab is in the process of fabricating 8.4 meter mirror segments for the Giant Magellan Telescope. Seven of the segments are off-axis with 14 mm of aspheric departure. In order to successfully fabricate these mirrors we are constantly taking steps towards faster, more deterministic methods, from diamond generating to stressed lap polishing. The Large Optical Generator (LOG) is celebrating its 30-year anniversary at the University of Arizona with a complement of technological updates and enhancements. This paper shows how some of these upgrades will aid in the manufacture of the GMT segments.

## 1. INTRODUCTION

The LOG is responsible for all diamond generating processes that take place at the Richard F. Caris Mirror Lab. The generating process bridges the gap between a rough cast mirror blank and fine grinding with the stressed lap. During the generating process a metal or resin bond diamond wheel grinds away at the substrate at removal rates upwards of 1.5 $cm^3$/sec. The rapid removal rate and accurate contouring of the machine enable an efficient removal of over 2400 kg from the front surface of the substrate, turning a rotationally symmetric cast surface into the highly aspheric prescription of a GMT off-axis segment. Once the surface has been generated to an accuracy of 10 to 20 µm RMS, the mirror is moved over to the Large Polishing Machine where the stressed lap, accompanied by fine abrasives, is used to achieve a smooth surface figure of 1 to 5 µm RMS. At this point polishing begins, guided by a complex optical test system consisting of two interferometers, a 4 m spherical fold mirror, a second 1 m spherical fold mirror and up to two laser trackers simultaneously. The mirror is complete when the customer-specified structure function is achieved, which typically requires a surface figure of 25 nm RMS or better.

The LOG was delivered to the College of Optical Sciences at the University of Arizona in July 1984, followed by installation and preliminary testing in late 1984 to early 1985. The first project the machine was intended for was the fabrication of a series of 2 m diameter off-axis mirror molds that would eventually be combined to constitute a 10 m sub-millimeter radio telescope[1]. The desired mirror mold accuracy was 3 µm RMS. In 1990 the LOG was moved to the Steward Observatory Mirror Lab, now known as the Richard F. Caris Mirror Lab, where it was intended to be used as both a diamond generating and polishing machine for mirrors up to 8.4 m in diameter.

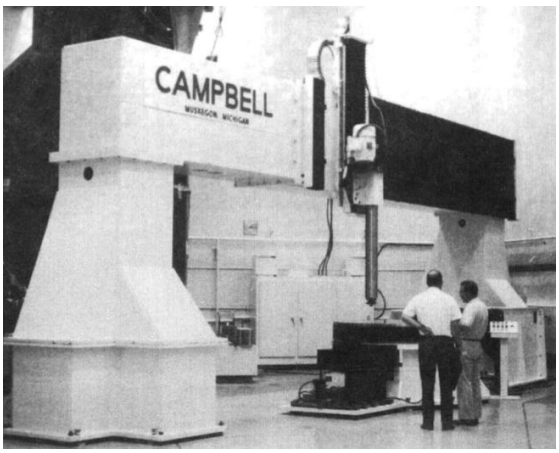


Figure 1: The LOG in the basement of the College of Optical Sciences, shortly after installation.

Optifab 2015, edited by Julie L. Bentley, Sebastian Stoebenau, Proc. of SPIE Vol. 9633, 96330Y

Since its early days at the Mirror Lab, the LOG has undergone several major upgrades, not including the upgrade currently underway. Each upgrade has been necessitated by the need either to replace out of date equipment or to add new critical functionality to meet the growing demands of ambitious telescope projects. The machine has been used not only for diamond generating, but also for polishing and figuring multiple mirrors to final specification by retrofitting it with a stressed lap polishing system.

In 2014 the latest of these upgrades, the most ambitious to date, began with the goal of adding entirely new electronics, motors, encoders, computing systems, software, metrology tools and many enhanced mechanical features. In Figure 2 the LOG is shown in its present configuration at the Richard F. Caris Mirror Lab.

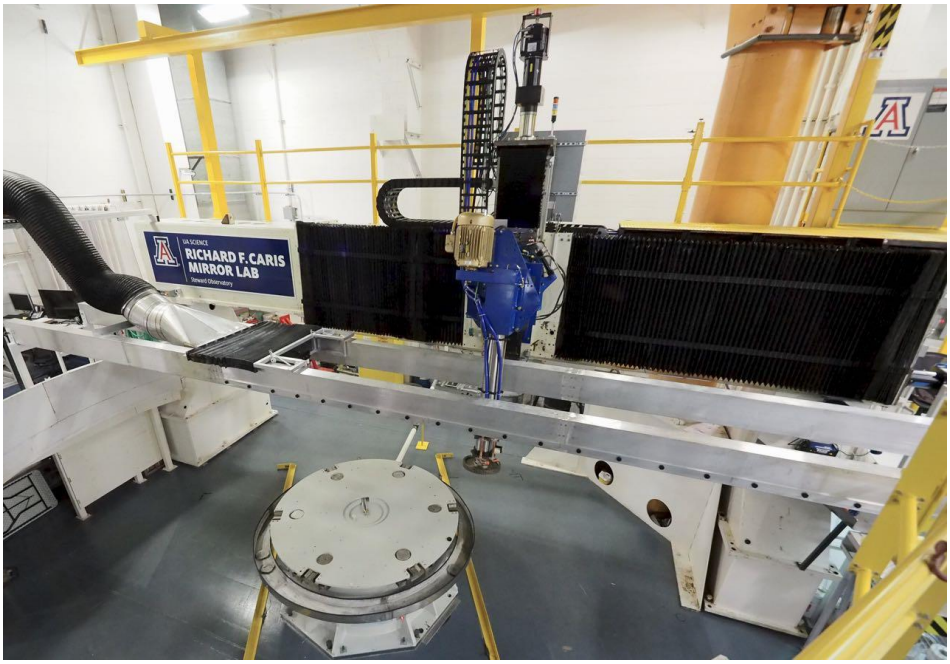


Figure 2: Some the latest additions are visible in this recent photograph, such as the vertical axis servo system, new positive air seal generating spindle and new VFD generating motor. Photo by Frank Gacon, Steward Observatory.

The new and improved LOG is now nearing completion with many of the new advanced features coming on-line and demonstrating very promising and long awaited capabilities. Some of the most exciting of these new capabilities are as follows:

- **AutoCal:** A method for calibrating a 5 m horizontal by 1 m vertical working envelope. We will discuss the metrology and software that enables 10 μm RMS profiling accuracy over the full envelope.
- **LOG+:** A method for converting the LOG into an in-situ, non-contact profilometer. We expect to achieve a full surface measurement accuracy of 5 to 10 μm RMS after calibration using the Mirror Lab's Laser Tracker Plus metrology system.
- **Directed Generating:** Software allows for surface measurements to be converted into generating hit maps along a configurable spiral path. As a result, new degrees of freedom for correcting high order surface errors have been enabled, with the intention of improving overall surface generating accuracy.

With the application of these and other innovations, our goal is to achieve a generated surface accuracy of 10 μm RMS or better on the GMT 8.4 m segments.

## 2. AUTOCAL ROUTINE

AutoCal is program that allows for a high-precision 2D calibration of the LOG. The software can command the machine to move in a number of modes while also recording encoder and motor information. Tool motion is monitored by a laser tracker. Using the automated motion and data recording properties of AutoCal with a FARO laser tracker, we are able to resolve errors down to a few microns over the large working envelope of the LOG. If the errors measured by the laser tracker are deemed repeatable, a look-up table is generated and used as a correction table in an effort to eliminate these errors. AutoCal also serves to evaluate the performance of the machine in terms of the servo tuning, motor current draw and mechanical soundness. By periodically running AutoCal we are able to track the performance of the machine over the long term and determine whether motor re-tuning or parts replacement or refurbishment is necessary.

In order achieve a true position tolerance of 10 μm RMS or better for every position of the generating spindle, we often employ two laser trackers simultaneously. By spacing the trackers at opposite ends of the machine's travel we can apply weighted biases to the raw data in order to create a more accurate measurement of the machine's large 5 m by 1 m working envelope. The laser trackers' retroreflectors are placed as close to the cutting point of the tool as possible. By doing so, we remove the need to evaluate the pitch, yaw and roll of the horizontal and vertical ways independently. All angles and non-linearities are conveyed as linear translations in X, Y and Z at the cutting location of the generating spindle.

To establish the coordinate frame from which we base our correction table for the machine, we use the turntable to define the Z-axis, which is nominally vertical. The X-axis of the coordinate frame for the AutoCal correction table is aligned to be parallel with the horizontal axis of the machine. The Y-axis runs in the other horizontal direction, perpendicular to the X-axis, following the right hand rule. The geometry of the machine has been made such that the generating spindle diamond wheel contact point is coincident with the Z-axis of the turntable when the horizontal axis is at a position of H = 0.

Both trackers must measure the turntable bearing radial and axial runout. The LOG turntable bearing has proven to be impressively smooth and axially flat during repeated measurements, both with and without loads up to 25,000 kg. The turntable bearing exhibits an axial runout, primarily astigmatic, of 60 μm PV at a radius of 1 m when unloaded. This astigmatic error is reduced when a load is applied. For example, we have found that the installation of a 6.5 m honeycomb mirror and cell, weighing about 25,000 kg, results in less axial runout, approximately 50 μm PV at a measuring radius of over 3 m. We attribute this effect to overcoming the bearing preload, which causes the bearing to warp when no load is applied. The radial runout is unaffected by loading the turntable and measures approximately 40 μm PV. The turntable bearing measurement results have demonstrated that a correction table for the turntable, as a function of angle, is unecessary. The smooth error of the bearing can be removed by applying a correction based on the measured surface error during the final stages of generating on the LOG.

Since the turntable defines the Z-axis, any motion of the turntable relative to the rest of the machine during installation of a mirror can result in the AutoCal correction table being rendered inaccurate. Considering that many of the optics that the Mirror Lab processes weigh in excess of 40,000 kg, shifting of the turntable is a very real possibility. For this reason we have evaluated the stability of the turntable with respect to the machine before and after a 25,000 kg test load has been installed. The results indicate an angular shift up to 0.0015°, relatively repeatable for a given load. This fact must be considered when an AutoCal correction table is created, with particular attention paid to the tilt of the X-Y plane about the Y-axis as this directly translates into a cone error in the mirror surface during generating.

The laser trackers that are used for the AutoCal routine have been verified to provide the accuracy necessary for our measurements, which is typically 30 to 40 μm at a distance of 5 m. The laser trackers are used exclusively in interferometric mode in an effort to achieve optimal distance measuring capability in the orientations in which the trackers are used. The accuracy of the measurements, for our application, is ultimately limited by the trackers' lateral (angular) coordinates, which are quoted to have a Maximum Permissible Error of 45 μm over the range of interest. In addition to verifying the trackers' measurement accuracy, we also verify their stability over time. These tests have revealed that some laser trackers are susceptible to encoder drift, which must later be compensated for or considered in the total error stack-up for an AutoCal routine. The two trackers used for the AutoCal results in this paper exhibited less than 10 μm RMS of positional drift at a distance of 4 m, over time spans of 10 hours or greater. In all, the primary errors to be considered for an AutoCal process can be distilled down to the values found in Table 1.

Table 1: Error sources considered in an AutoCal routine. Estimated laser tracker errors are based on the manufacturer's Maximum Permissible Error and field tests at the Mirror Lab.

| **Error source** | **Maximum expected error for any position in the full machine working envelope (μm)** | **Error magnitude can be reduced by simultaneous measurement with a second laser tracker? (YES/NO)** |
|---|---|---|
| Laser tracker systematic errors, including encoder drift | < 35 | YES |
| Laser tracker measurement noise | < 25 | YES |
| Thermal perturbations in the lab (thermal variation is ±0.5 °C) | < 10 | NO |
| LOG linear encoder feedback latency for scanning data acquisition | < 10 | NO |
| Horizontal linear encoder errors | < 4 | YES |
| Vertical linear encoder errors | < 2 | YES |

By acquiring between two and eight horizontal scans and between two and eight vertical scans, with two different trackers simultaneously, we expect to provide an average error plot of the machine's encoders with a true position accuracy of 25 μm or better for any point in the machine envelope.

Our acquisition type is a complementary mixture of two approaches. The first part consists of high resolution linear scans on both axes independently, with a point sampling of approximately 10 mm for the horizontal axis and 0.5 mm for the vertical axis. The second acquisition part consists of medium resolution grid scans with a point sampling every 50 to 100 mm. The grid scan reveals cross-talk between the axes that would otherwise go unnoticed during our high resolution scans of one axis. We have found that the data from a grid scan and from the high-resolution line scans agree nicely. For this reason we rely more heavily on the grid scan and interpolate between the points. This approach results in faster data acquisition without degradation in accuracy.

AutoCal also has the provision for conducting both stable-point and continuous-scan measurements. The advantage of the stable-point technique is that it removes the introduction of encoder readout latency errors. For a continuous scan we are forced to limit the scanning speed due to these latency errors. The drawback for stable-point data acquisition lies in the fact that the machine must start and stop for each position, which is unlike the more continuous motion used on the LOG during generating operations.

## 3. MACHINE ERRORS WITH RESPECT TO THE GMT OFF-AXIS PRESCRIPTION

Our selection of which errors to evaluate is primarily driven by the prescription for a GMT off-axis segment[2]. The GMT parent is a near-paraboloid with R = 36 m and D ≈ 25 m. The segment is 8.4 m in diameter and 8.71 m off-axis. In Figure 3 we see the aspheric departure of a GMT off-axis segment with piston, tip, tilt and power removed.

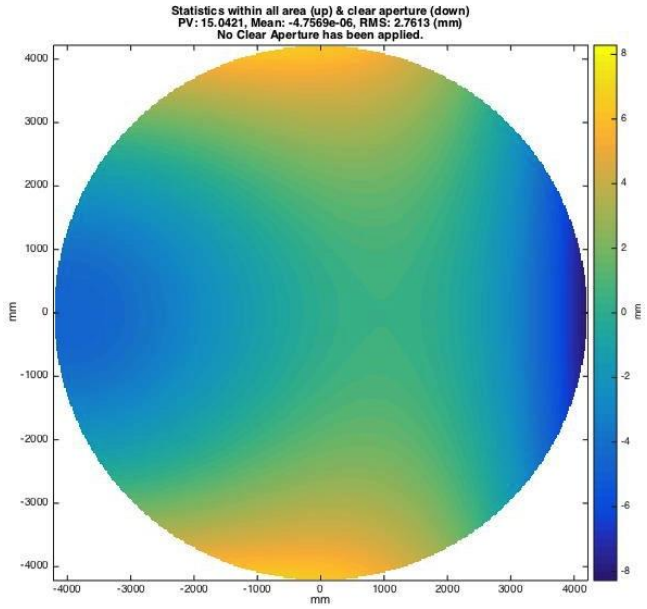


Figure 3: Surface map of a GMT off-axis segment. The parent vertex is to the left. Piston, tip, tilt and power have been removed in order to show the aspheric departure more clearly.

The largest sensitivities to machine errors are based on the most significant slopes on the mirror. In the case of a GMT off-axis segment the greatest slopes are at the outer edge of the mirror, the largest slope component being in the radial direction as a result of the parent optic curvature. The maximum slope is 1 in 8.8, or 6.5°. This ratio gives the sensitivity of the surface error to horizontal position error. Because of the asphericity, radial slopes along the X and Y axes are slightly different, but we ignore the difference for the sensitivity analysis.

As can be seen in Figure 4 the sagitta of the mirror is approximately 240 mm with the highest radial slopes located at the outer diameter.

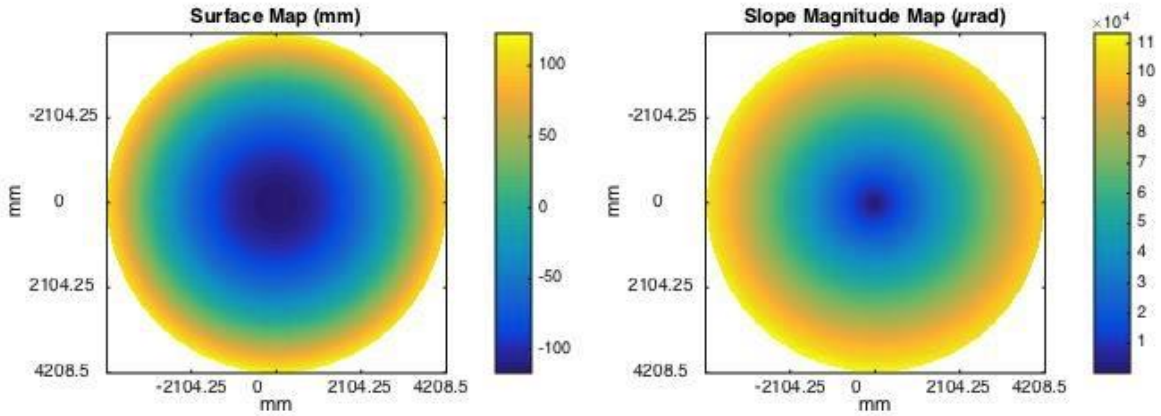


Figure 4: The sagitta of a GMT off-axis segment is approximately 240 mm, while the maximum radial slope is approximately 110 mrad or 6.5°.

The second most significant slope component is tangent to the outer diameter of the mirror, along the Y-axis of the machine coordinate system. The aspheric departure includes 14 mm PV astigmatism at the outer diameter of the mirror. The maximum slope magnitude in the tangential direction is 0.24 mm per degree of turntable motion. For this reason, the angular error of the turntable must be kept within ±0.04° in order to avoid worst case surface height errors greater than

10 μm. Y-axis displacements from the motion of the horizontal and vertical axes can also translate into a surface height error. For this reason we verify that Y-axis displacements of the diamond tool are less than ±0.15 mm in order to keep the resultant local surface error well below 5 μm. If we find that the Y-axis does not deviate by more than this amount we have no need to create a correction table for Y-axis perturbations as a function of horizontal and vertical axis motion. Figure 5 shows the slopes in the tangential direction.

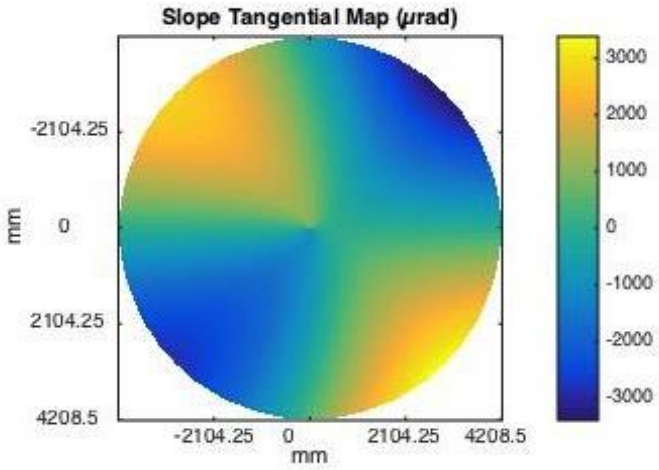


Figure 5: Slopes in the tangential direction.

Now that the coupled effects of each axis with respect to the mirror prescription have been considered we can formulate a simple error budget. For the purposes of purely considering the calibration of the horizontal and vertical axes we will assume that the turntable angular error is well below the ±0.04° limit. The total complement of these errors is considered in Table 2.

Table 2: Surface height errors as a function of various axis position errors.

| Error source | Maximum allowed position error for axis, locally (μm) | Maximum sensitivity of surface height to position error | Maximum surface height error (μm) |
|---|---|---|---|
| Vertical vs. Vertical | ± 10 | 1 : 1 | ± 10 |
| Vertical vs. Horizontal | ± 20 | 1 : 1 | ± 20 |
| Horizontal vs. Horizontal | ± 25 | 1 : 8.8 | ± 3 |
| Horizontal vs. Vertical | ± 25 | 1 : 8.8 | ± 3 |
| Y-Axis vs. Vertical | ± 500 | 1 : 301 | ± 2 |
| Y-Axis vs. Horizontal | ± 500 | 1 : 301 | ± 2 |

Not all errors can be considered in terms of their local contribution to the surface error. In the case of a non-orthogonality between the vertical and the horizontal axes, a 0.05° angular error, for example, results in a sag error of 25 μm. Most of the sag errors that are the result of smooth low order errors over the full range of motion of either the vertical or horizontal axes are relatively small in magnitude and very repeatable. We expect that the application of directed generating, to be discussed in Section 6, will correct whatever smooth low order sag errors make it past our AutoCal calibration. Even so, we set upper bounds for the maximum allowed error over the full range of motion for each axis, shown in Table 3.

Table 3: Sag errors that are the result of non-orthogonalities between axes and other low order effects.

| Error source, linear or second order | Error limit for full range of motion necessary for generating a GMT off-axis segment (μm) | Resultant sag error (μm) |
|---|---|---|
| Vertical vs. Vertical | 25 | 25 |
| Vertical vs. Horizontal | 50 | 50 |
| Horizontal vs. Horizontal | 50 | 6 |
| Horizontal vs. Vertical | 150 | 17 |
| Y-Axis vs. Vertical | 1000 | 3 |
| Y-Axis vs. Horizontal | 1000 | 3 |

## 4. AUTOCAL MEASUREMENT RESULTS

The AutoCal scan results presented in this section were taken over the course of three weeks spanning April and May 2015. We start by investigating the error plots for vertical vs. vertical, vertical vs. horizontal, horizontal vs. horizontal and horizontal vs. vertical. Our measurements have indicated that errors along the Y-axis as a function of both the vertical and horizontal axes were well below our error budget value; therefore they will not be covered in further detail.

The vertical vs. vertical measurement, shown in Figure 6, displays a quadratic error as a function of vertical position. We found that this was almost entirely attributed to the bowing of the vertical ways as the slide traverses from top to bottom. We would have to go to extensive lengths to stiffen the vertical ways to eliminate this error were it not for our ability to measure and compensate for highly repeatable errors.

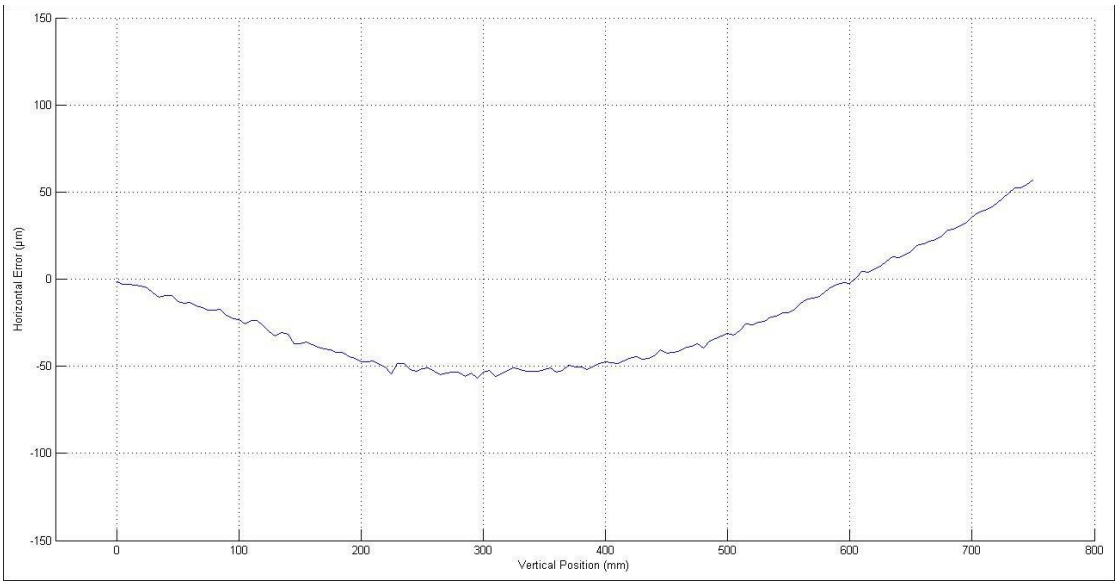


Figure 6: Average error for vertical vs. vertical from three scans with two trackers simultaneously, no calibration.

The vertical vs. horizontal measurement, shown in Figure 7, displays non-linearities in the horizontal ways as well as a tilt error present between the turntable bearing and the horizontal axis. If the turntable bearing tilts during mirror loading, the resultant error will show a linear term for vertical vs. horizontal. An angular shift of 0.001° translates into 73 μm of cone error in the mirror surface.

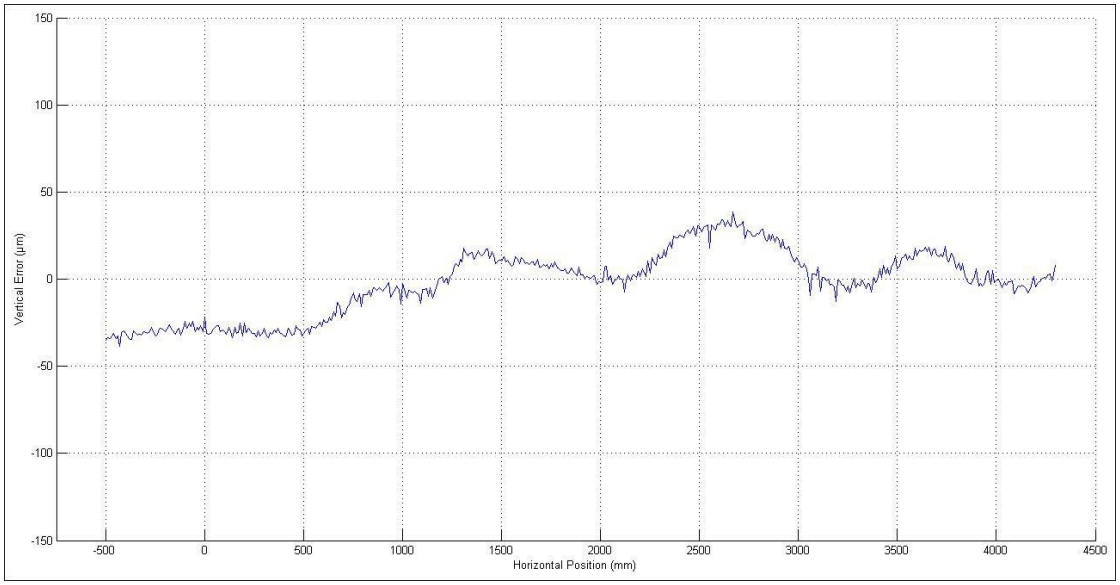


Figure 7: Average error for vertical vs. horizontal from three scans with two trackers simultaneously, no calibration.

The error from the horizontal vs. horizontal measurement, Figure 8, is primarily the result of the pitch and yaw errors in the motion of the horizontal slide along the horizontal ways. The diamond generating tool is displaced from the encoder read head location by approximately 1 to 2 m, depending on vertical position. As a result the pitch and yaw errors present in the horizontal ways partially manifest as linear displacements along the X-axis at the generating wheel location.

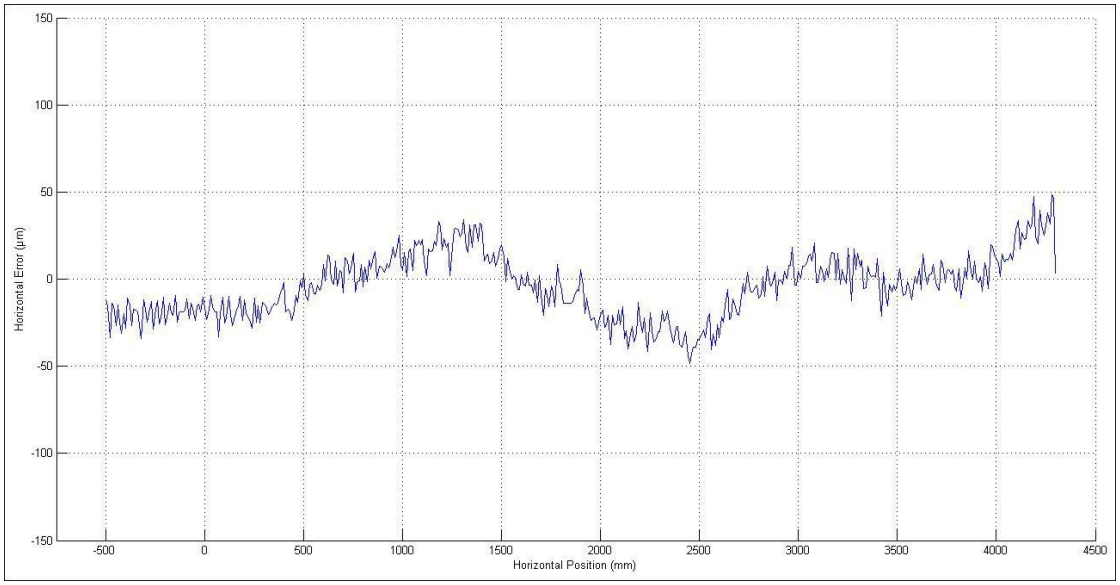


Figure 8: Average error for horizontal vs. horizontal from three scans with two trackers simultaneously, no calibration.

The last measurement to consider, shown in Figure 9, is horizontal vs. vertical. In general we avoid applying a horizontal vs. vertical correction if the error is considered negligible, the goal being to reduce the overall complexity of the calibration table. As can be seen in Figure 9, the total magnitude of the error is approximately 0.1 mm and even less for

the sub-range of the vertical axis that will be used for generating a GMT segment. The total sag error, as a result of the horizontal vs. vertical dependence, is less than 11 µm.

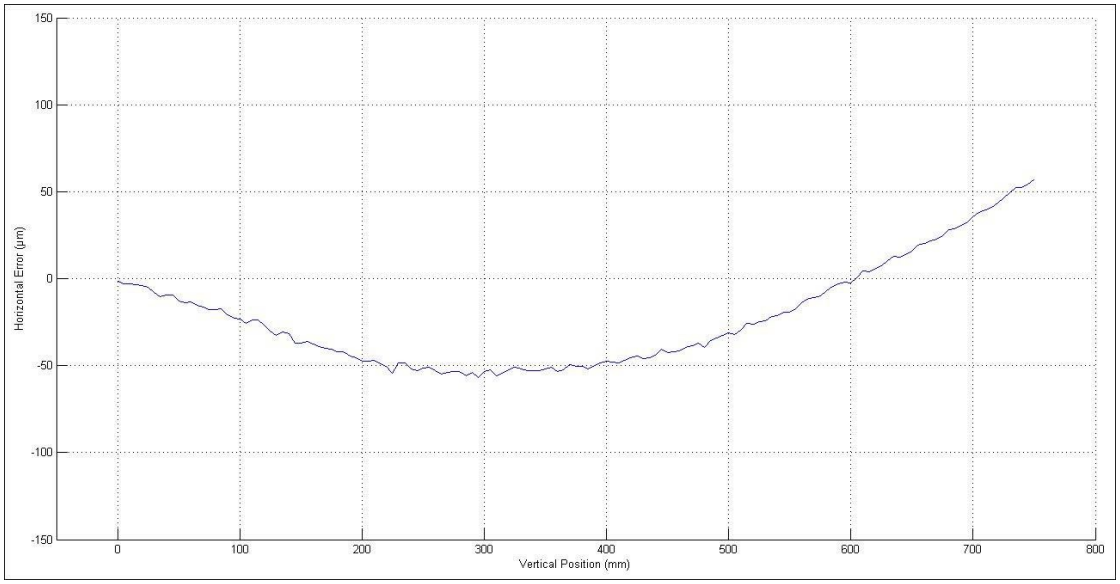


Figure 9: Average error for horizontal vs. vertical from three scans with two trackers simultaneously, no calibration.

Once the AutoCal measurements have been performed we can create a 2D machine calibration look-up table. The error magnitude and direction derived from the AutoCal measurements can be found in Figure 10, where we have provided a downsampled representation. When we generate, the 2D calibration table is used to correct tool position errors by interpolating between the laser tracker measurement locations and subtracting the measured error from the desired position to get the commanded position for the horizontal and vertical axes.

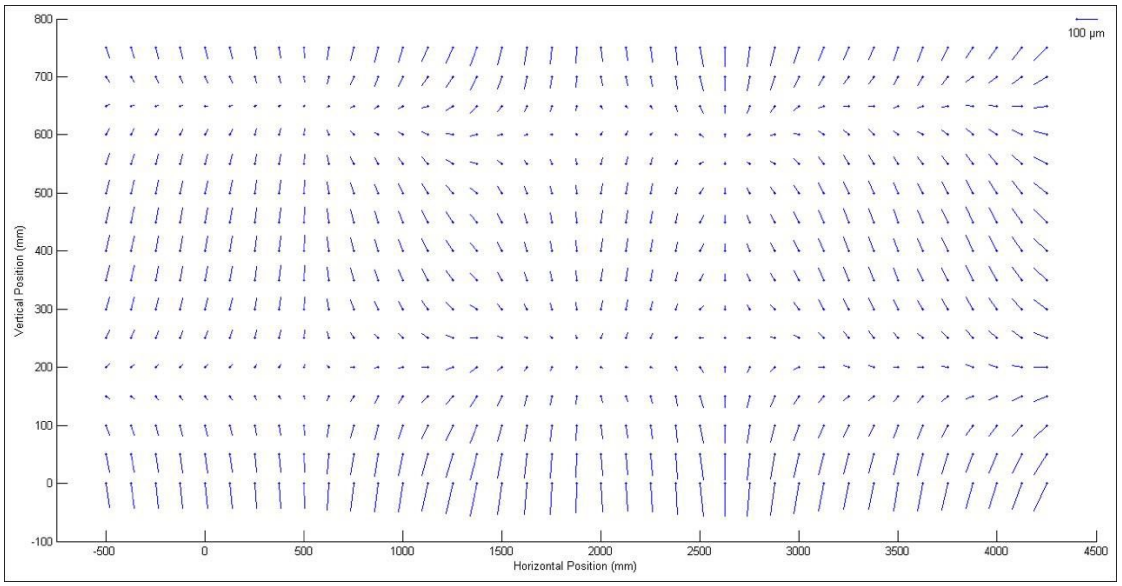


Figure 10: Axis corrections from the calibration look-up table, shown here sampled every 125 mm in horizontal and every 50 mm in vertical.

The 2D calibration look-up table is applied and a second AutoCal routine is performed in order to verify the effectiveness of the calibration table. If all the errors measured from the first AutoCal routine were 100% repeatable we would see perfect correction. However, due to coordinate frame shifts, laser tracker non-repeatabilities and machine non-repeatabilities, we only achieve a partial correction. We observe a substantial reduction in the original errors, often by a factor of two to three. In Figure 11, for example, we see a substantial improvement in vertical vs. vertical after the calibration table has been applied. The original 260 μm PV quadratic error has been removed and replaced with a relatively flat error and only small local variations. Our specification of ±10 μm for any given position on the vertical axis has been met over a 750 mm range of travel, which is more than three times the vertical axis motion necessary to accommodate the 240 mm sag of a GMT off-axis segment.

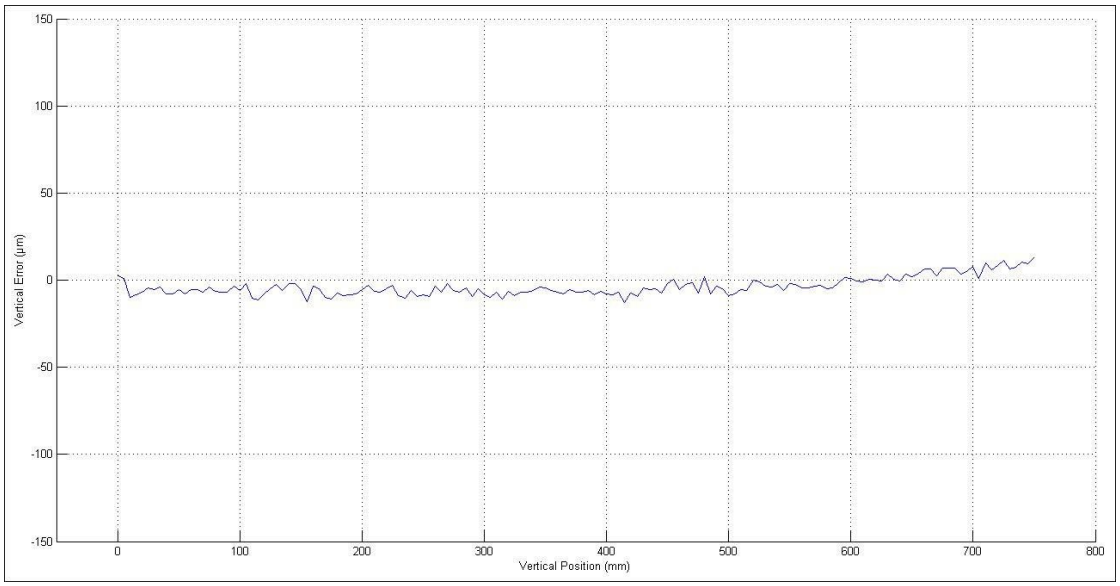


Figure 11: Average error for vertical vs. vertical from three scans with two trackers simultaneously, calibration applied.

In Figure 12 we examine the vertical vs. horizontal data with the calibration table applied. The large bumps that were originally located at 1500 mm and 2600 mm have been reduced to fine-scale residual structure. The peak to valley of these local structures has been reduced from approximately 45 μm to 25 μm and the global tilt has been reduced from approximately 60 μm to 40 μm. The vertical vs. horizontal data demonstrates that we meet our error budget allowance, described in Tables 2 and 3.

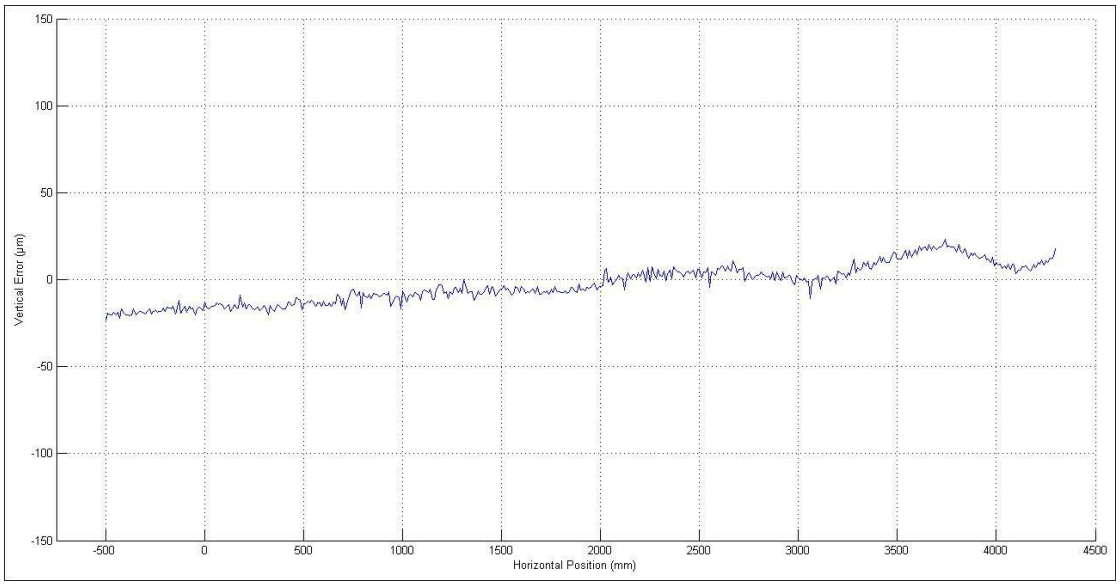


Figure 12: Average error for vertical vs. horizontal from three scans with two trackers simultaneously, calibration applied.

In Figure 13, we observe a nice improvement in the horizontal vs. horizontal error. What was originally a 100 µm PV error with large low order structures is now a very flat error with only a 40 µm PV error, not counting the 35 µm error at the outermost horizontal position.

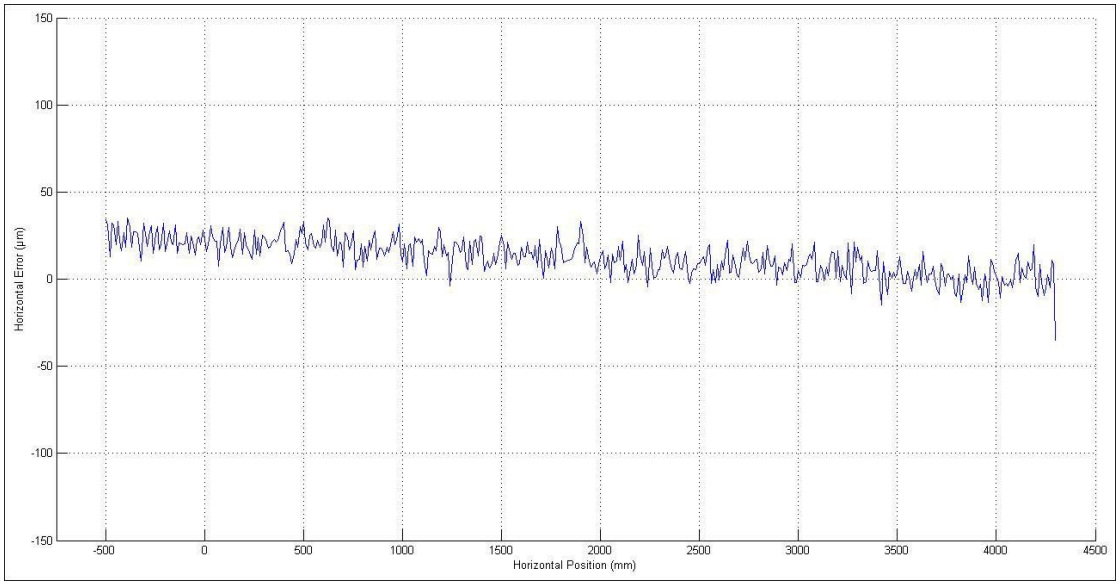


Figure 13: Average error for horizontal vs. horizontal from three scans with two trackers simultaneously, calibration applied.

When we consider all of the residual errors remaining, taking into account the relative weighting from Table 2, we find that the AutoCal 2D calibration table has provided us with an excellent starting point for accurately generating a GMT off-axis mirror. Our measurements have indicated that errors in the motion of the machine are repeatable and can be removed by actively correcting with encoder offsets. All of the errors fall within the error budget presented in Tables 2 and 3 by a comfortable margin. The next task is to establish an accurate and efficient method for measuring a generated surface, followed by a method for actively controlling the convergence of a mirror during fine diamond generating.

## 5. DESCRIPTION AND PLANNED IMPLEMENTATION OF LOG+

One of the biggest challenges we face at the Mirror Lab on a routine basis is coordination and implementation of optical testing. Accurate measurement of mirror surfaces at the Mirror Lab is carried out under the test tower, located several meters from the LOG. Moving a 40,000 kg mirror and cell combination followed by precise optical test alignment is no small feat. In addition, minimizing the number of moves between the LOG and the test tower can significantly reduce the total generating time. For this reason, developing an in-situ metrology technique on the LOG that provides very accurate, full surface information is ideal. In this section we will discuss how we intend to use the LT+ system to calibrate an in-situ, non-contact, full surface profilometry system on the LOG, called LOG+.

Fundamentally, there is nothing novel about the technology that goes into the LOG+ system. The foundation of what makes the system work, which is very similar to most high precision CMMs on the market today, consists primarily of seven features:

1. Independent measurement system used as the reference standard which can provide an accurate calibration method for resolving systematic errors in the LOG+ system.
2. Ensure all axes being used in the measurement have highly repeatable motion characteristics and accurate encoding with 0.5 to 1.0 μm resolution.
3. Non-contact measurement probe with a 1 μm measurement accuracy or better, which is minimally affected by slopes in the radial and/or tangential direction.
4. Precise and systematic way of referencing the optic with respect to the machine and the independent test system.
5. Stable test environment with thermal perturbations not exceeding ±0.5 °C and minimal vibration.
6. Stable support system for the mirror, where varying support forces contribute less than 5 μm RMS in surface error.
7. Smooth generated test surface that minimizes measurement noise.

The independent measurement, feature 1, is provided by the Mirror Lab's Laser Tracker Plus system (LT+), which combines a commercial laser tracker with several enhancements that improve accuracy for measuring a mirror surface[3]. The laser tracker uses a distance-measuring interferometer (DMI) and angle encoders to measure the position of a retroreflector in spherical polar coordinates. We scan the retroreflector over the mirror surface with an air-bearing puck and measure 200 to 250 points in about 45 minutes. The most important enhancement of LT+ is adding stability references that allow us to measure rigid-body motion of the mirror or the laser tracker, typically several microns during the scan. We measure these drifts by mounting another DMI on the same platform with the laser tracker and continuously monitoring four retroreflectors placed every 90° around the edge of the mirror. With this information we can correct for changes in piston, tip and tilt of the mirror relative to the laser tracker. The accuracy is also enhanced by measuring with the tracker's beam roughly normal to the mirror surface—so the surface height depends most strongly on the tracker's more accurate line-of-sight coordinate—and performing a custom calibration of the less accurate angular coordinates. LT+ has an accuracy better than 2 μm RMS as demonstrated by comparison with optical interferometer measurements.

We perform occasional LT+ measurements, compare them with the LOG+ measurements, and use the difference to make a correction table for LOG+. This approach provides us with a way to correct systematic errors in the LOG+ system, such as axial runout in the turntable bearing.

Our AutoCal measurements have demonstrated the ability to remove repeatable errors in the motion of the LOG horizontal and vertical axes for simple linear motions. Calibration with LT+ goes further to remove errors that may depend on the specific tool path used to contour the prescription of an 8.4 m GMT off-axis segment, which encompasses 14 mm of aspheric departure and 240 mm of sag. It also removes repeatable errors that do not come directly from tool motion, such as errors related to wear of the diamond wheel or deflection of the mirror and/or tool under load. Both AutoCal and calibration with LT+ depend on feature 2, repeatable motion and accurate encoding.

We can illustrate the importance of feature 4, accurate registration of the mirror for both LOG+ and LT+ measurements, by considering a rotational mismatch between data sets. If a 0.05° rotational mismatch occurs, we incur an astigmatic error of 5 μm RMS, as can be seen in Figure 14. This amount of rotational mismatch between the two data sets equates to a 3.7 mm tangential displacement at the outer circumference of the mirror. We use alignment references on the mirror to orient the coordinate frames of both data sets to better than 1 mm. Other sources of alignment error include colocation of the center of the optic for both measurement system coordinate frames, which can lead to incorrect measurements of power, astigmatism and coma.

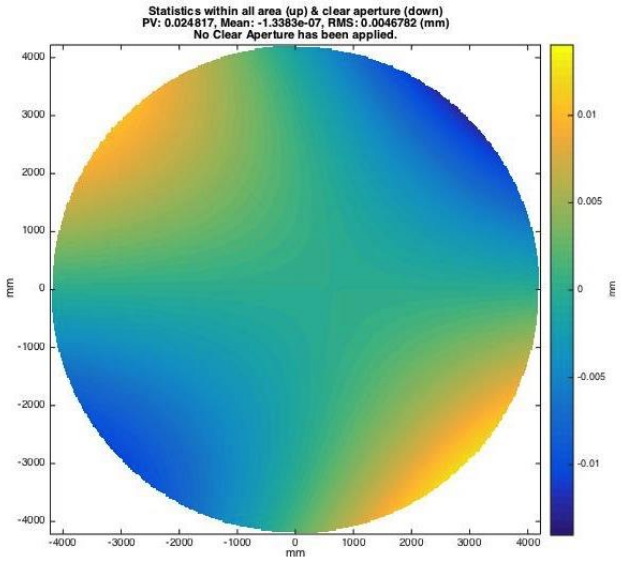


Figure 14: Surface error created by a 0.05° rotational mismatch between LOG+ and LT+ data sets.

Features 5 and 6 are coupled. Thermal perturbation in the lab can affect both the support system and the mirror. Thermal variations within the mirror substrate can lead to low order effects, such as power, astigmatism and trefoil, as well as high order effects that may or may not have rotational symmetry. The mirror is most sensitive to front-to-back gradients: a 1 K temperature difference leads to 13 μm RMS of power. We must thermally equilibrate the mirror prior to a LOG+ or LT+ measurement if we want to minimize these errors. The mirror support system is also sensitive to temperature variations as well as changes in the way the support cell is mounted. We expect the support-induced surface errors to be less than 5 μm RMS. If necessary, we can characterize them and correct for them.

Finally we consider features 3 and 7 together, as they are also coupled. We have selected a Keyence laser triangulation sensor based on the results produced by the swing-arm profilometers used in the College of Optical Sciences optical shop. A 1.2 m mirror was recently completed using this configuration, along with an interferometric null test for verification purposes. The agreement between the profilometer system and the interferometric null test confirmed that the selected probe provides more than enough accuracy for our needs on the LOG+ system. The accuracy of the selected measurement probe is rarely the limiting factor; variations in support forces and calibration of measurement system geometries more often lead to low order measurement discrepancies. Surfaces with a micro-roughness of 0.5 to 2 μm RMS, which correspond to a diamond particle size of 30 to 150 μm, are routinely measured with this type of probe without any significant degradation to measurement accuracy. As one would expect, there is a relationship between surface micro-roughness and measurement noise. Our final generating process, Micro Diamond Finishing (MDF), produces a micro-roughness of about 0.5 μm RMS and does not limit the measurement accuracy of the Keyence probe.

When we consider all the benefits associated with in-situ metrology on the LOG, the justification for LOG+ is apparent. The spatial resolution for measurements using this system will be four to six times that of the LT+ system. We accomplish this by rotating the turntable during a profile measurement, which effectively traces out a spiral path on the surface of the mirror. Measurements are entirely non-contact, which reduces the likelihood of scratches and other surface imperfections. By reducing the number of moves between the LOG and the test tower we reduce the total processing time as well as minimize the frequency of mirror moves, which pose a risk and require extensive supervision. In addition, limiting the number of measurements using LT+ to a few per mirror frees up the test tower for optical testing of other mirrors that are concurrently being processed on the Large Polishing Machine. Finally, we can create an efficient and robust feedback loop using LOG+ measurements and generating hit maps. By integrating our measurement and generating software into one system we are able to streamline the process and reduce reliance on additional mechanical, electronic and software sub-systems.

## 6. DIRECTED GENERATING USING SAGUARO HIT MAPS

Over the past three decades the LOG has provided very good generating performance on mirrors ranging in diameter from 2 m to 8.4 m[4]. Surfaces with 20 to 30 μm RMS accuracy have routinely been achieved using a relatively simple spiral path that follows the optical prescription of the mirror. The degrees of freedom for influencing the shape of the mirror during generating have been limited to radius of curvature, a few low-order aberrations, effective diamond wheel radius, and cone error, the latter of which can be controlled by shifting the zero point of the machine's horizontal axis. We have never had the ability to directly correct high order surface errors with or without rotational symmetry, until now. By combining high spatial resolution measurements and new software, we are able to command the servo system to directly control the shape of the mirror based on measured surface errors.

The use of measured surface errors to modify the tool path, which we call directed generating, is implemented in the SAGUARO software platform developed at the University of Arizona College of Optical Sciences[5]. The inputs for creating a directed generating run in SAGUARO can be split into two elements:

- **Machine run parameters:** These are used to generate a spiral path for the tool over the mirror surface and include variables such as surface feed rate (mm/sec), maximum depth of cut (mm), spiral pitch (mm/revolution of turntable), diamond wheel type, spindle speed (rpm) and spiral start and end radii (mm).
- **Surface error map:** The surface error map is created using LOG+ or LT+ data and provides vertical corrections. The corrections may be some percentage of the total surface error, as opposed to a full correction.

The surface error map is a summation of a number of contributing factors that may have different sources such as tool wear, axial turntable bearing runout, residual motion errors that were not accounted for in AutoCal, and thermal expansion of the generating spindle.

Once the directed generating hit map file has been created in SAGUARO, it is exported to the LOG control software where the mirror coordinates in the run file are converted to turntable and horizontal axis positions. The vertical corrections from the hit map file are summed with the mirror surface height to create the final vertical axis position information. This method allows us to visualize the subtle corrections that may change from run to run. The overall mirror prescription, which is static, constitutes the majority of the vertical axis motion over the course of a generating run.

In Figure 15, a 3D plot shows the vertical corrections that are applied to the tool position, for a surface error map that exhibits non-rotationally symmetric errors. The spiral path of the tool is defined using the machine run parameters in the SAGUARO module. In this case the spiral pitch was set to 100 mm/rev, which is uncharacteristically coarse, in order to show the tool path more clearly.

Most of the generating time on the LOG is spent conducting bulk material removal. We expect to use directed generating only with the finest diamond wheel. As can be seen in Table 4, we estimate that directed generating runs will account for around 25% of the total processing time. During the final stage our goal is to achieve a surface accuracy of 10 μm RMS or better, accompanied by approximately 0.5 μm RMS surface finish. Achieving this level of accuracy in the generating process will minimize the time to be spent fine grinding with the 1.2 m stressed lap.

Table 4: Estimated time spent for each generating step along with the estimated surface error.

| Generating process | Estimated process time, including metrology (hours) | Target surface accuracy (μm RMS) |
|---|---|---|
| 60/40 mesh metal bond cup wheel | 350 | 125 |
| 120 mesh resin bond cup wheel | 150 | 40 |
| Micro Diamond Finishing (MDF) using directed generating, with 30 μm diamond resin bond cup wheel | 180 | 10 |

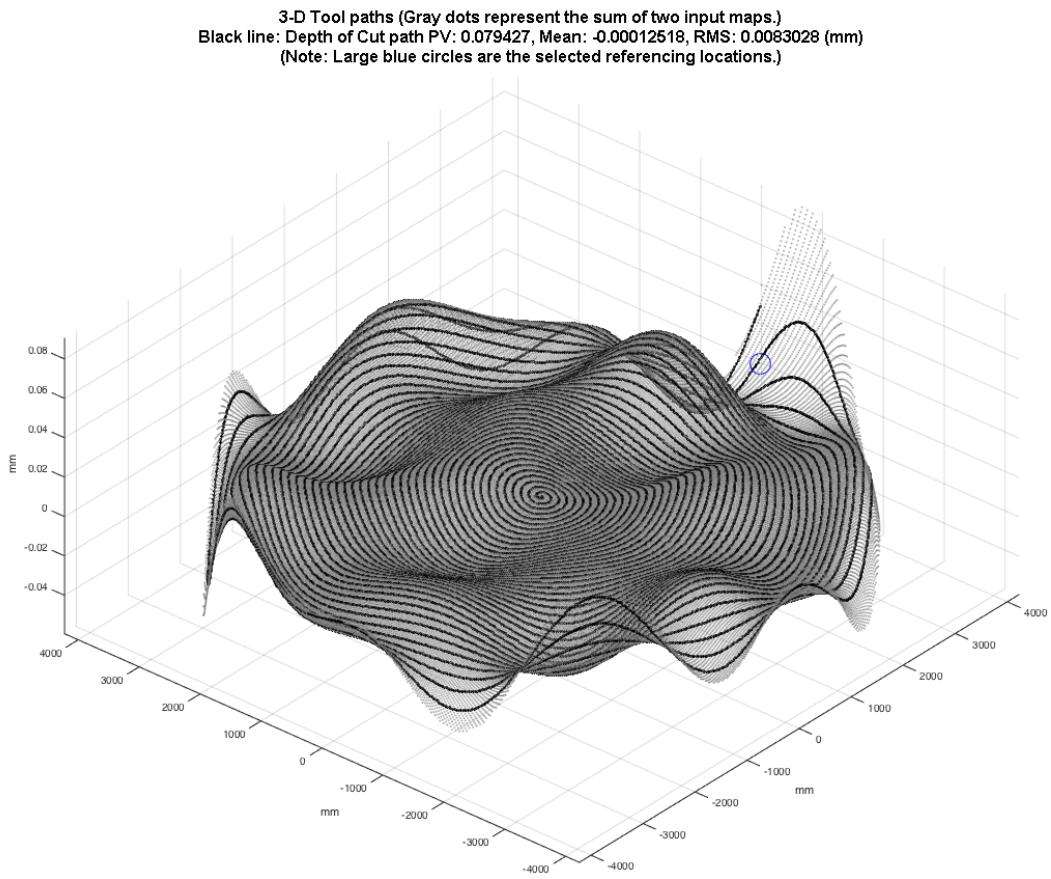


Figure 15: 3D plot showing the spiral path overlaid on a SAGUARO hit map.

## 7. CONCLUSION

We have presented three new capabilities that are being added to the LOG during its current upgrade. AutoCal now provides a comprehensive tool for evaluating and correcting repeatable errors in the horizontal and vertical axes of the machine. The proposed LOG+ system promises new advances in streamlining the measurement process for front surface generating. New degrees of freedom for controlling surface error using directed generating are planned, enabling us to reduce high order errors based on surface measurements made with LOG+ and LT+. By implementing all of these features on the LOG we expect to achieve a surface accuracy of 10 μm RMS or better on the remaining GMT segments to be processed by the Mirror Lab. In addition, the new capabilities will reduce the processing time for each mirror in order to provide the GMT project with excellent mirrors in a time frame consistent with the telescope construction schedule.

## ACKNOWLEDGEMENTS

This work has been supported by the GMTO Corporation, a non-profit organization operated on behalf of an international consortium of universities and institutions: Astronomy Australia Limited, the Australian National University, the Carnegie Institution for Science, Harvard University, the Korea Astronomy and Space Science Institute, the Smithsonian Institution, the University of Texas at Austin, Texas A&M University, the University of Arizona and the University of Chicago.

## REFERENCES


[1] R.E. Parks, P. Lam and W. Kuhn, "The large optical generator: a progress report", *Optical Fabrication and Testing Workshop: Large Telescope Optics*, Proc. SPIE 542 (1985).

[2] H.M. Martin, R.G. Allen, J.H. Burge, D. Kim, J.S. Kingsley, K. Law, R. Lutz, P.A. Strittmatter, P. Su, M.T. Tuell, S.C. West and P. Zhou, "Production of 8.4 m segments for the Giant Magellan Telescope", in *Modern Technologies in Space- and Ground-based Telescopes and Instrumentation*, ed. R. Navarro, C. Cunningham and E. Prieto, Proc. SPIE 8450, 84502D (2012).

[3] T.L. Zobrist, J.H. Burge and H.M. Martin, "Accuracy of laser tracker measurements of the GMT 8.4 m off-axis mirror segments", in *Modern Technologies in Space- and Ground-based Telescopes and Instrumentation*, ed. E. Atad-Ettedgui and D. Lemke, Proc. SPIE 7739 (2010).

[4] D.A. Ketelsen, W.B. Davison, S.T. DeRigne and W.C. Kittrell, "A machine for complete fabrication of 8-m class mirrors" in *Advanced Technology Optical Telescopes V*, ed. L.M. Stepp, Proc. SPIE 2199 (1994).

[5] G.A. Smith, B.J. Lewis, M. Palmer, D. Kim, A.R. Loeff and J.H. Burge, "Open source data analysis and visualization software for optical engineering", in *Novel Optical Systems Design and Optimization XV*, Proc. SPIE 8487, 84870F-1 (2012).